Defence Science Journal, Vol. 71, No. 3, May 2021, pp. 403-409, DOI : 10.14429/dsj.71.16110

Multi-mode Resonator based Concurrent Triple-band Band pass Filter with Six Transmission Zeros for Defence/Intelligent Transportation Systems Application

Shivesh Tripathi[#,*], B. Mohapatra[@], Prabhakar Tiwari[$], and V.S.Tripathi[&]

[#]*Department of Electrical and Electronics Engineering, Galgotias College of Engineering and Technology, Greater Noida - 201 310, India*

[@]*School of Electrical, Electronics and Communication Engineering, Galgotias University, Gautam Buddha Nagar - 201 306, India*

[$]*Department of Electrical Engineering, MMM University of Technology, Gorakhpur - 273 016, India*

[&]*Motilal Nehru National Institute of Technology, Prayagraj - 211 004, India*

[*]*E-mail: shiveshtripathi@gmail.com*

ABSTRACT

A compact and highly selective triple-band bandpass filter (BPF) is designed and presented in this paper. Proposed filter offers low insertion loss, and passband characteristics is achieved by using two coupled MMR multi-mode resonators (MMR1 and MMR2) and an inverted T and circular shape MMRs. The filter operates at frequency 2.43 GHz (Vehicular Communication), 5.91 GHz (ITS band), and 8.86 GHz (satellite communication band). The simulation and measurement results show a minimum insertion loss of 1.6 dB, 0.73 dB, and 2.8 dB for triple-band BPF. The return loss is found to be greater than 13.06 dB, 28.6 dB, and 21.55 dB. It is noted that measurement results are in accordance with the result of electromagnetic simulation. Desired triple-band multi-mode resonators (MMRs) filter characteristics are achieved with six transmission zeroes (TZs). The filter comprises of MMRs which provide small size and control over the spurious frequency. By using a parallel-coupled microstrip line, the first and third passbands are realised. Whereas by using an end-coupled microstrip line, the second passband is recognised. At the input and output ports, the resonator coupling technique is used. By using the anti-parallel microstrip line arrangement, the transmission zero is acquired. The dimensions of the designed filter are 25×16 mm 2.

Keywords: Bandpass filter; Even and odd mode microstrip coupled line; Multi-mode resonators; Six transmission zeroes filter; Triple-band filter

1. INTRODUCTION

In the era of the internet of things (IoT), various machine to machine (M-2-M) communication applications require a multiband operation to communicate in different bands like ITS, Vehicular Communication, and satellite communication band. Intelligent transportation system (ITS) goal is to attain traffic efficiency by reducing traffic problems. The main objective is to reduce the time spent by the commuters also protecting their safety and comfort. ITS applications are globally accepted and are being used in many developed countries. A microwave filter is an essential building block of the communication system. It is used in mobile communication, sensors, radar, satellite communication and vehicular communication systems. A good microwave filter should have sharp frequency-selectivity, insertion loss, and return loss. It should have good impedance matching with joined components. As shown in Fig. 1, information and communication systems are integrated into the transport infrastructure and vehicles in order to reduce transportation time, fuel consumptions keeping human safety. ITS supports vehicle accident avoidance, automatic toll collection, vehicle navigation, etc. It comprises vehicle to vehicle, vehicle to infrastructure and vehicle to satellite communications.

Received : 09 July 2020, Revised : 18 October 2020
Accepted : 09 December 2020, Online published : 17 May 2021

The filter can be characterised by reflection and transmission coefficients, which can be expressed in polynomial terms that contain all information about poles and zeros of the filter. There are many ways for the physical realization of filter, but network design theory is almost the same to all. A bandpass filter (BPF) using a microstrip structure has a simple design, lightweight, and low cost. A microstrip BPF can be easily integrated with the front end of the transmitter. An MMR is used as a non-uniform transmission line resonator, and its application to BPF with the stripline construction is reported in[1-2]. *In*[3] Bandpass and the hairpin resonator is used for RF receiver front end for intelligent transportation systems (ITS). A triple-band BPF with better selectivity based on modified grounded MMR has been given in[4]. *In*[5] a microwave front-end design of adaptable BPF and filtenna, for GPS and ITS application have been reported. An analytical approach for designing the resonator is presented in[6]. *In*[7] the filters are realized using parallel connected micro strip line and end coupled micro strip line. *In*[8] a compact dual-band BPF using embedded spiral resonator is reported. A compact tri-band BPF based on λ/4 resonator having advantages in terms of the independent design is reported in[9]. A double mode resonator with four square patches and a micro strip circle resonator has been presented in[10-11]. MMR based advanced triple-band BPF is reported in[12-13]. A compact triple-band high-temperature superconducting filter is presented in[14].

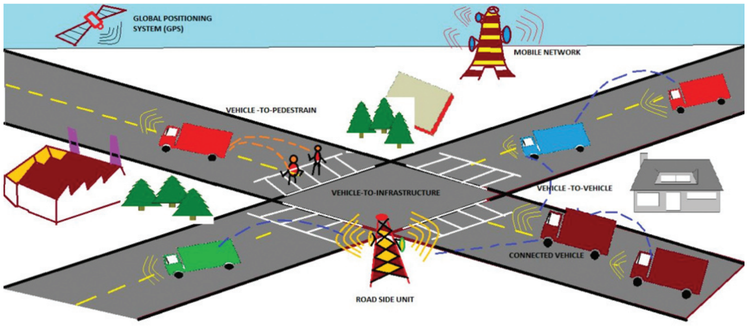

Figure 1. Application of ITS.

The suggested filter used a multimode stub-loaded resonator suitable for ISM band, WLAN, WiMAX application. A set of dual- and triple-band BPF employing equal-length coupled-serial-shunted lines have been presented in[15-16]. *In*[17] a shunt open stub-loaded open-loop resonator has been introduced to construct a double band BPF. Multi-mode resonators based triple-band BPF with off-band characteristics has been described in [18]. Different filter architectures for triple-band BPF design have been suggested for ITS and general communication[19-28].

This paper demonstrates a new method to design a coupled MMR-based concurrent operation triple-band BPF with six TZs. This filter is realized using T- inverted and circular-shaped MMR. Due to the identical construction of MMR, the even and odd mode techniques are used for study of the filter. The offered three resonant frequencies. Simulation of the filter is carried out employing Ansoft HFSS V.16 and manufactured on Rogers-4350 substrate. The dielectric constant of the substrate is €r= 3.38 and 1.524 mm in thickness. Due to which the filter is very small. Measured results validates the simulated results of the proposed BPF for DSRC/ITS application.

2. TRIPLE BAND MICROSTRIP BPF DESIGNAND ANALYSIS

2.1 Geometry and Design of Structure

The concept of an MMR was originated and extended to the implementation of triple-band BPF. It is designed by providing the primary few resonant frequencies into the specified wide passband and putting in place the coupling peak of the parallel-coupled lines at the centre frequency. Finally, we demonstrate the triple band pass filter style that offered with the sensible in-band transmission, improved out-of-band rejection, and excited band-notch theoretically and by experimentation. Therefore, the analysis is oriented to achieve the following:

(i) Resonators Lightweight.
(ii) Poor coupling between resonators while maintaining relatively low spacing.
(iii) In the design phase, unnecessary parasitic couplings may be overlooked, because beyond the nearest neighbouring resonators, the resonator gets much less parasitic coupling.
(iv) To keep the BW and passband shape almost constant.
(v) Microwave filter have been developed from some nonlinear materials, such as superconductors, to produce intermodulation (IMD) deformation.

The flow chart of the CAD-based filter and another component design using waveguide has been shown in Fig. 2. The general synthesis procedure has been discussed. The basic general approach is used in the design of the BPF. A microstrip parallel-coupled MMR based concurrent triple-band BPF has been fabricated. The BPF has six TZs. The initial structure of the inverted T-shaped MMR is shown in Fig. 3. By using a mix of interdigital input/output coupled lines, it can realize a variety of possible applications. The proposed resonator is symmetrical in structure. The design was performed in Rogers RT/Duroid material with substrate thickness (H) = 1.524 mm, €r= 3.38, and tanδ = 0.0025. The proposed filter is designed to bandpass triple bands at 2.43 GHz (2.4GHz - 2.6 GHz) for vehicular communication band, 5.91 GHz (5.73-6.0GHz) for DSRC/ITS applications, and at 8.86 GHz (8.4 GHz - 10.1

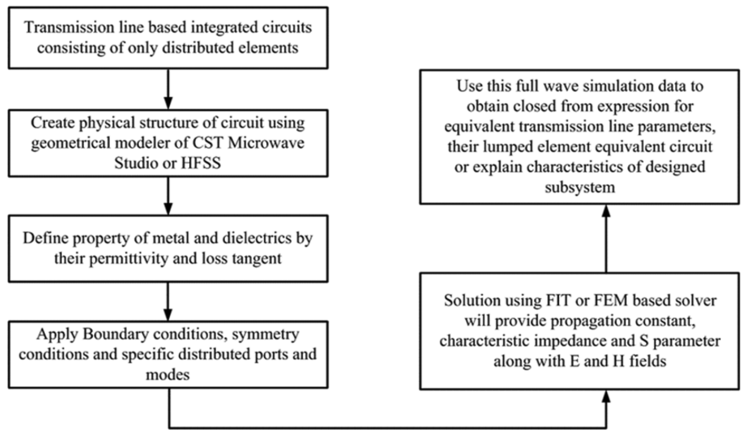

Figure 2. Flow chart of CAD-based passive rf circuit design approach.

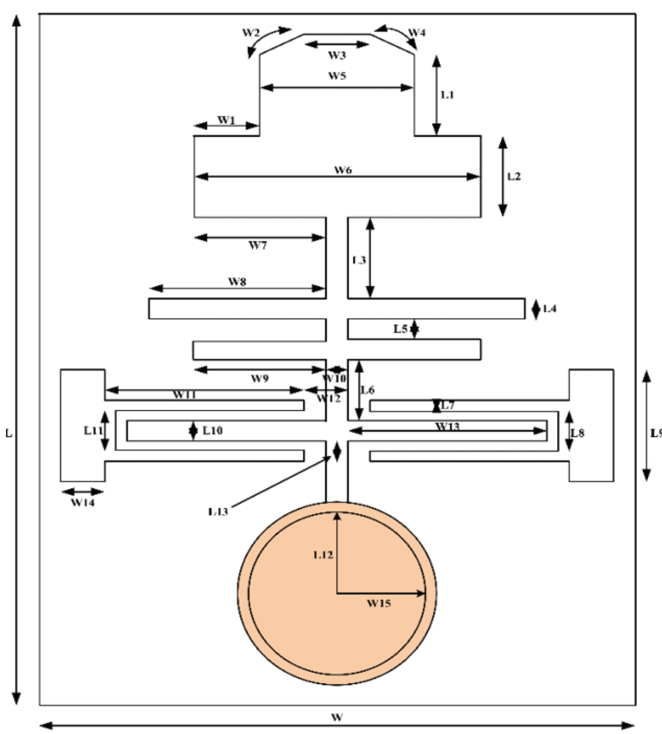

Figure 3. Configuration of the triple band BPF.

GHz) for satellite communication. The top portion of MMR is the inverted T shaped; the middle portion of the filter is inter digitized coupled and the lower portion of MMR is a circular ring. The top and the middle portion of MMR is responsible for matching the input port to the output port, and the lower portion of MMR results is a triple band.

In order to realize the excellent performance at the given triple-band center frequencies and filter bandwidths, the parameters i.e. input/output port width (W14), coupled line length (W11), input/output coupled-line width (L7), interstage coupled-line length (L6), input/output coupled-line spacing (W12), circle radius (L12), and width (W15) have been correctly optimized. 2 microstrip lines with a characteristic impedance of fifty Ω are used to supply the planned coupling filter. Table 1 indicates the dimension (in mm) of the proposed triple-band microstrip BPF.

Table 1. Triple band pass filter

Parameters	Values (mm)	Parameters	Values (mm)	Parameters	Values (mm)
L1	3.18	L7	0.4	L13	0.75
L2	2.26	L8	1.1	L	25
L3	2.64	L9	3.6	W	16
L4	0.5	L10	0.5	W5	4
L5	0.37	L11	0.7	W6	8
L6	2.37	L12	3.5	W7	3.75
W15	4	W1	2	W8	6.2
W9	2.2	W12	1	W10	0.49
W14	1	W13	6.5	W11	6.5
W2	1.32	W3	1.36	W4	1.32

2.2 MMR Characteristics and TZs

The physical structure of MMR is symmetrical. So even and odd mode analysis can be used for resonance analysis.

$$Y_{even} = Y_{odd} = 0 \tag{1}$$

where Y_{even} is the admittance of even mode structure and Y_{odd} is the admittance of odd mode structure. Figure 4 depicts the simulated resonating modes of the resonators. To obtain three passbands in the designed BPF, two types of MMRs are used. To resonate at 2.43 and 8.86 GHz the upper portion of MMR is designed and for resonance at 5.9 GHz, circular-shaped MMR is designed. Remaining parts of the resonator is used for impedance matching.

Figure 5. (a) portrays the corresponding transmission line mannequin of the MMR in even and odd mode. It is evident in Fig. 5 (b) that even-mode resonant frequencies are fixed, but the odd mode resonant frequency is barely moved with the variant in the gap between the resonator and the interdigital connector (L11). For each of the even and odd modes, the simulated resonant peaks correlate with the analytic choices. Figure 5 (a) depicts the estimated transmission line circuit models for odd and even mode excitation. Here $\Theta_{M,} \Theta_{ST1,} \Theta_{ST2}$ refer to electrical lengths, and Y_M, Y_{ST1}, Y_{ST2} refer to the characteristic admittance of the width.

The input admittances $Y_{i\ even}$ of the even mode resonators can be explained as follows:

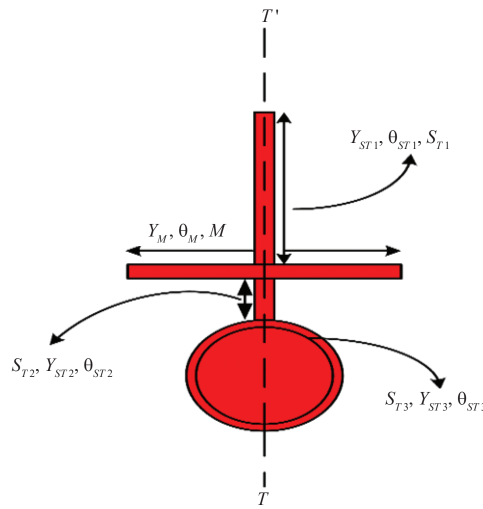

Figure 4. The geometry of circular MMRs.

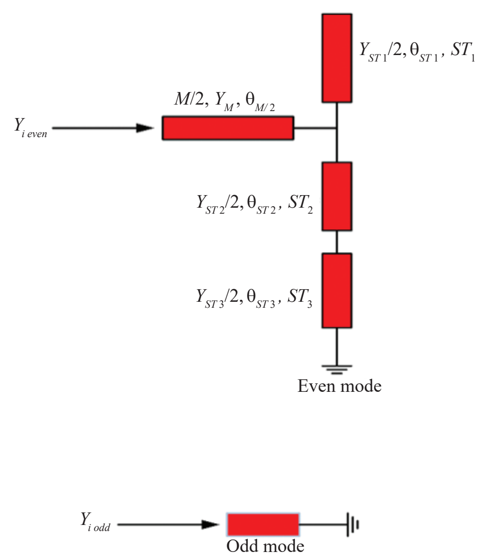

(a)

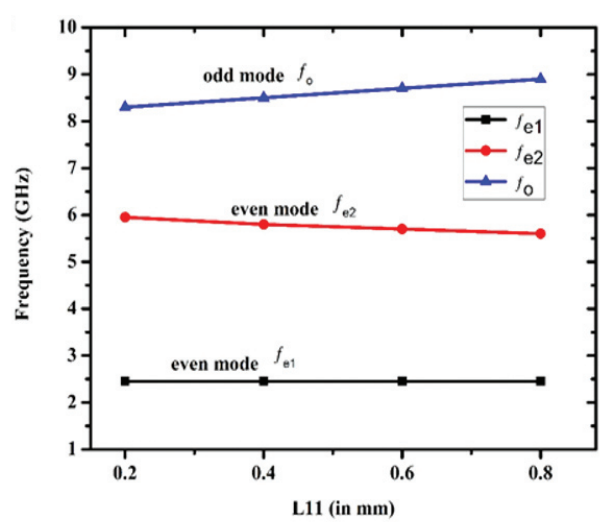

(b)

Figure 5. (a) Even and odd mode equivalent transmission line models (b)|S21| weakly coupled even and odd mode triple band BPFF.

$$Y_{ieven} = Y_M \frac{Y_{ieven1} + jY_M \tan(\theta_M / 2)}{Y_M + jY_{ieven1} \tan(\theta_M / 2)} \qquad (2)$$

where

$$Y_{ieven1} = Y_{ieven2} + j\frac{Y_{ST1}}{2}\tan(\theta_{ST1}) = Y_{ieven2} + \frac{1}{2}jY_{ST1}\tan(\theta_{ST1}) \qquad (3)$$

$$Y_{ieven2} = \frac{j\frac{Y_{ST2}}{2}\left[\frac{Y_{ST2}}{2}\tan(\theta_{ST2}) + \frac{Y_{ST3}}{2}\tan(\theta_{ST3})\right]}{\frac{Y_{ST2}}{2} - \frac{Y_{ST3}}{2}\tan(\theta_{ST2}).\tan(\theta_{ST3})} \qquad (4)$$

and

$$Y_{ieven2} = \frac{j\frac{Y_{ST2}}{2}\left[Y_{ST2}\tan(\theta_{ST2}) + Y_{ST3}\tan(\theta_{ST3})\right]}{\left[Y_{ST2} - Y_{ST3}\tan(\theta_{ST2}).\tan(\theta_{ST3})\right]} \qquad (5)$$

The odd mode resonators $Y_{i\ odd}$ can be explained as follows:

$$Y_{iodd} = Y_M \frac{Y_{iodd1} + jY_M \tan(\theta_M / 2)}{Y_M + jY_{iodd1} \tan(\theta_M / 2)} \qquad (6)$$

where

$$Y_{iodd1} = -j\frac{Y_{ST2}}{2}\cot(\theta_{ST2}) + Y_{iodd2}$$

$$Y_{iodd1} = Y_{iodd2} - \frac{1}{2}jY_{ST2}\cot(\theta_{ST2}) \qquad (7)$$

$$Y_{iodd2} = j\frac{Y_{ST1}}{2}\frac{\frac{Y_{ST1}}{2}\tan(\theta_{ST1}) - 1}{\tan(\theta_{ST1}) + \frac{Y_{ST1}}{2}}$$

$$Y_{iodd2} = jY_{ST1}\frac{\left[Y_{ST1}\tan(\theta_{ST1}) - 2\right]}{2\left[2\tan(\theta_{ST1}) + Y_{ST1}\right]} \qquad (8)$$

where M is the physical length of the resonator, Y_M is the admittance of resonator, Θ_M is the electrical length of the resonator, $ST1$ is given as the physical length of stub 1, Θ_{ST1} is the electrical length of stub 1, Y_{ST1} is the admittance of stub 1, $ST2$ is the physical length of stub 2, Θ_{ST2} is the electrical length of stub 2, Y_{ST2} is the admittance of stub 2. For even mode at resonance,

$$f_{even} \cong \frac{2mc}{(M + ST_3)\sqrt{\varepsilon_{eff}}} \qquad (9)$$

where m = 1, 2 and c is the speed of light. For odd mode at resonance,

$$f_{odd} \cong \frac{c}{(ST_1 + ST_2)\sqrt{\varepsilon_{eff}}} \qquad (10)$$

For the extraction of coupling coefficients, Fig. 6 represents the EM simulated frequency response. The filter is studied due to the symmetrical nature of the even and odd mode analysis of the resonator. A coupling coefficient at the resonant frequency of two identical equivalent standard microstrip resonators was considered. Where the effective dielectric constants for even and odd modes in coupled microstrip lines are resonant frequency. Using a weakly coupled resonator, even and odd modes are analyzed. The even-odd mode of the loose coupling is used with variation in L_{11} to find even and odd mode of the filter. Structure of the resonator is symmetrical about TT'. In the odd mode, the load is grounded at mid-point and in even mode load is open circuited at mid-point. Even mode resonant frequencies are fixed when increasing the value of $L_{11,}$ whereas odd mode resonant frequencies are varied in accordance with values of L_{11}.

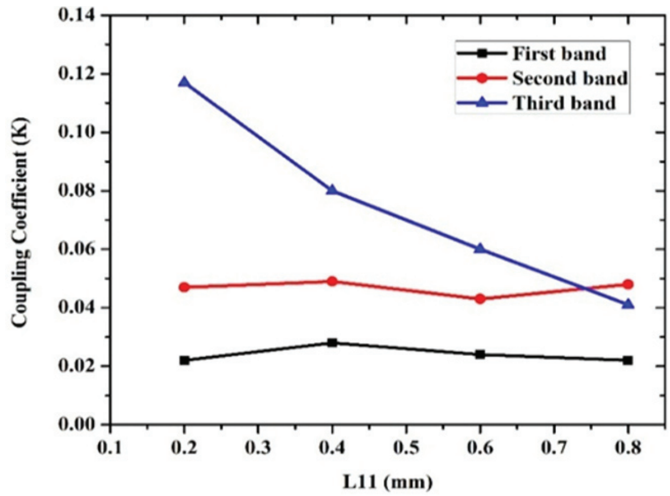

Figure 6. EM simulated frequency response for the extraction of coupling coefficients.

$$Q_e = \frac{f_o}{\Delta f} \qquad (11)$$

$$\Delta f = f_+ - f_- \qquad (12)$$

where $f_{o=}$ Centre frequency, Δf is bandwidth, f_+ and f_- are the frequencies when the phase is $\pm 90°$ with respect to f_o.

The coupling coefficient and external quality factor Qe of this filter are dependent on parameter W_{15} as shown in Fig. 7. Also, the parameter W_{15} determines the bandwidth of all the pass bands assist variation causes the change in the external quality factor of the proposed filter as predicted from Fig. 7.

In addition, Tzs is a frequency at which there is zero propagation of the transfer function of a linear two-port network. Tzs at zero frequency and infinite frequency may be found in HPF and LPF respectively. Transfer functions with both zero and infinite frequency can be found in BPF. Six TZ's three bands are obtained in the planned BPF. Depending on the size of the perturbation factor, the position of the two transmission zeros is determined using a simple transmission-line model.

3. SIMULATION AND MEASUREMENT RESULTS

A triple-band BPF is designed and configured using HFSS to validate the idea of the proposed filter and the S-parameters are calculated using a vector network analyzer (VNA). Figure 8 shows the fabricated structure.

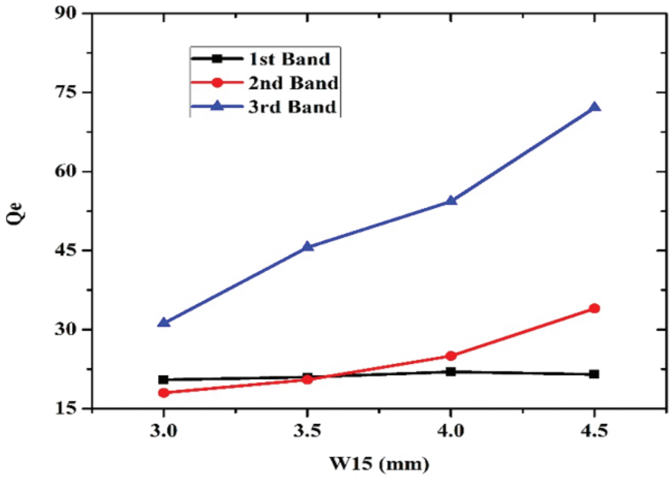

Figure 7. Extracted quality factor (Qe) of the triple-band BPF.

Figure 9(a) displays the simulated and calculated |S11| of the planned filter. It is found that the first band has a return loss of 13.06 dB, the second -28.6 dB and the third has loss of -21.55 dB. Triple bands below -10 dB level are reached by the proposed filter. Figure 9(b) displays the simulated and measured triple band bandpass filter |S21|. The minimum measured insertion losses, including losses from 2 SMA connectors, were found to be 1.6, 0.73 and 2.8 dB within the 3 passbands. Figure 8(c) shows the simulated and estimated S-parameters of the proposed filter. It is accomplished in three

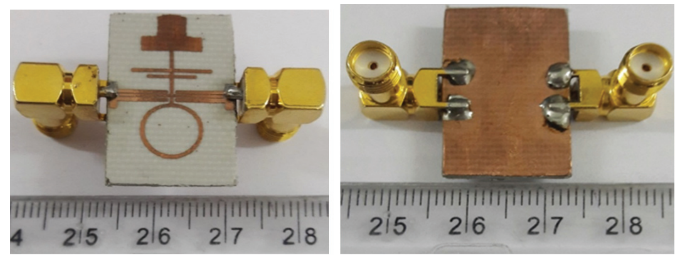

(a) (b)

Figure 8. Fabricated triple band BPF (a) top view, (b) a bottom view.

bands with resonant frequencies of 2.43 GHz (2.4-2.6GHz), 5.91 GHz (5.73-6.0GHz), and 8.86 GHz (8.4 GHz - 10.1 GHz). These bands, respectively, are beneficial for vehicular communication, ITS and satellite communication.

Six transmission zeroes gives better selectivity to this filter between the triple bands and rejects undesired frequencies. The first transmission zero is obtained at 1.71 GHz, second at 3.7 GHz, third at 5.2 GHz, fourth at 6.46 GHz, fifth at 7.4 GHz and sixth at 12.4 GHz. Figure 10 depicts the electric current distribution of the triple band BPF at different resonant frequencies. Figure 10 (a) depicts that upper portion of the resonator is applicable for 2.4 GHz band. Figure 10(b) shows that all parts of the resonator are responsible for 5.9 GHz, and Fig. 10(c) shows that some of the upper and lower parts of the resonator are responsible for the 8.8 GHz higher frequency band. Finally, Table 2 provides a comparison of the

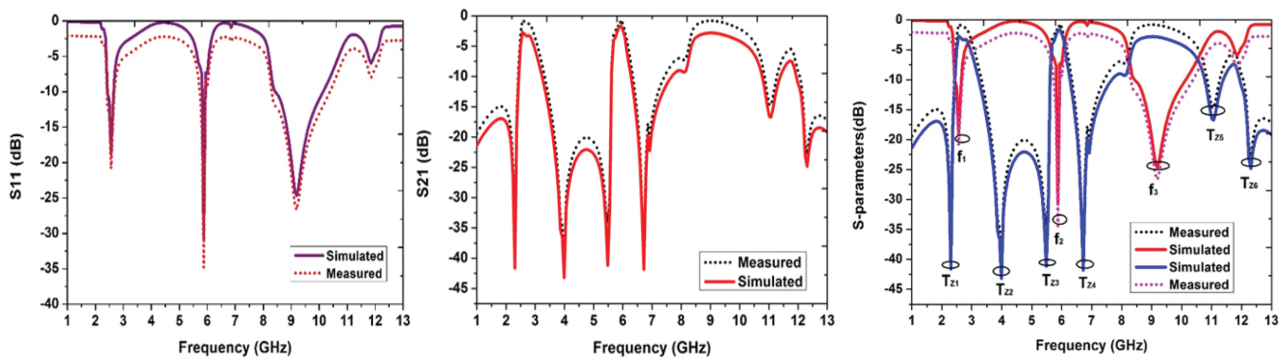

(a) (b) (c)

Figure 9. (a) Simulated and measured Triple band BPF return losses (b) Show Triple band BPF transmission characteristics (S21) (c) Simulated and measured BPF triple band S-parameters.

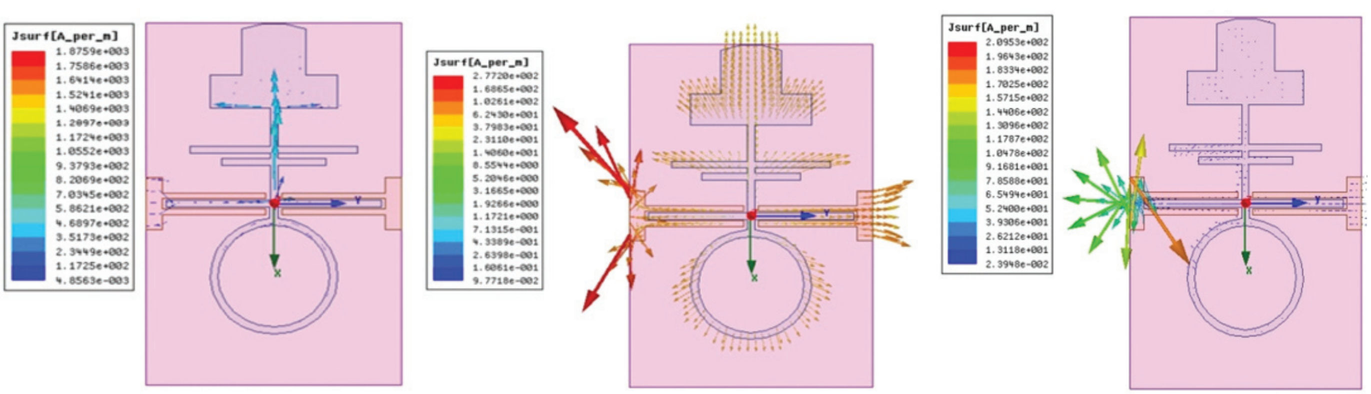

(a) (b) (c)

Figure 10. Electric current distribution of the proposed filter at different resonant frequencies. (a) 2.4 GHz band. (b) 5.9 GHz band 10 (c) 8.8 GHz band.

Table 2. Performance comparison with other BPF

Reference	Centre frequency (GHz)	Insertion loss (IL)(dB)	Return loss (RL) (dB)	No. of transmission Zeroes (Tzs)	Size (mm)	Fractional bandwidth
[4]	3.48/4.18/5.25	1.53/ 2.11/ 2.65	15.1/ 22.8/ 19	5	18.4 × 9	7 %, 5 % and 6 %
[6]	2.4/ 3.8/ 5.7	0.82/2.0/2.5	20/22/18.2	3	19 × 8.6	7.5 %, 3% and 4 %
[9]	1.8 / 3.5 / 5.8	0.88/ 1.33/ 1.77	21.3/15.84/15.72	3	27 × 11.7	7.0%, 5.0% and 3.5%
[13]	2.35/4.78/ 7.21	1.0/0.6/2.37	24/14/10	5	14.36 × 7.03	7.1%, 7.1% and 5.5%
[14]	2.45/3.5/5.2	0.16/ 0.55/ 0.22	16.7/10.2/ 17.5	5	8.3 × 8.6	9.7%, 5.1% and 1.9%
[27]	2.4/3.2/4.3	1.68/1.65/1.5	6/7/8	3	44 × 50	7 %, 7.5 %, and 5 %
This Work	2.43/5.91/8.86	1.6/0.73/2.8	13.06/28.6/21.55	6	25 × 16	8.23%,4.56% and 9.18%

proposed work with the research on triple band BPF previously reported. It clearly shows the better performance of the work done in current reported paper, which makes it more fit for ITS applications.

4. CONCLUSIONS

We proposed a novel BPF structure having three band of operation in this paper. The filter uses an inverted T and circular shaped MMR. Moreover the filter passband is obtained at the frequency of 2.43 GHz, 5.91 GHz, 8.86 GHz. The insertion loss is reported to be less than 1.6 dB, 0.73 dB and 2.8 dB at respective bands. The desired triple band multi-mode resonator (MMRs) filter has been obtained with six transmission zeros (TZ). These are compact MMR filters, which control small size and characteristic frequency. Three bands are obtained in the filter, the first band is found suitable for vehicle communications, the second for ITS applications and the third band for defense applications. The above results show that the filter is well suited for Defence/ITS applications. In the future, this MMR filter will be used to build an integrated communication system for automobiles, using our own custom subsystem for transceiver modules.

REFERENCE

1. Haldar MK; Farzamnia A; Su HT. Multimode resonator microstripbandpass filters. *In I2CACIS*, 2017, 52-55. doi: 10.1109/I2CACIS.2017.8239032.
2. Xiao; J. K.; Li; Y; Zu, X; P. & Zhao; W. Multi-mode multi-band bandpass filter using hexagonal patch. resonator. *IJE*, 2015, **102**(2), 283-292. doi.10.1080/00207217.2014.896048
3. Lai; W. C.; Huang, J.-F.; & Yang, P.-G. Design of RF receiver front-end with bandpass and hairpin resonator narrow band filter for high speed intelligent DSRC application. *In ICCP, IEEE,* 2014, 1222–1229. doi: 10.1109/ICCPS.2014.7062218
4. Mo, Y; Song, K; & Fan, Y. Miniaturized triple-band bandpass filter using coupled lines and grounded stepped impedance resonators. *IEEE MWCL*, 2014; **24**(5), 333-335. doi: 10.1109/LMWC.2014.2310458
5. Tripathi, S; Pathak, NP; & Parida, M. Microwave front-end subsystems design for ITS/GPS applications. *ESTIJ*, 2016, **19**(4), 1815-1825. doi: 10.1016/j.jestch.2016.08.017
6. Guan, X; Ma, Z; & Cai P. A novel triple-band microstrip bandpass filter for wireless communication. *MOTL,* 2009; **51**(6),1568-1569. doi: 10.1002/mop.24382
7. Kuo, YT & Chang, CY. Analytical design of two-mode dual-band filters using E-shaped resonators. *IEEE Trans. Microwave T.Techn.,* 2012, **60**(2), 250-60. doi: 10.1109/TMTT.2011.2176506
8. Luo, X; Qian, H; Ma, JG; Ma, K; & Yeo, KS. Compact dual-band bandpass filters using novel embedded spiral resonator (ESR). *IEEE MWCL,* 2010, **20**(8), 435-437. doi: 10.1109/LMWC.2010.2050195
9. Zhang, S & Zhu, L. Compact tri-band bandpass filter based on λ/4 resonators with U-folded coupled-line. *IEEE MWCL,* 2013, **23**(5), 258-260. doi: 10.1109/LMWC.2013.2255868
10. Zhang, XY; Chen, JX; Xue, Q; & Li, SM. Dual-band bandpass filters using stub-loaded resonators. *IEEE MWCL,* 2007, **17**(8), 583-585. doi: 10.1109/ISAPE.2010.5696697
11. Gorur, A. Description of coupling between degenerate modes of a dual-mode microstrip loop resonator using a novel perturbation arrangement and its dual-mode bandpass filter applications. *IEEE Trans. Microwave T. Techn.,* 2004, **52**(2), 671-677. doi: 10.1109/TMTT.2003.822033
12. Li, JJ; Wang, GY; & Chen, CF. Compact triple-wideband bandpass filter based on multi-mode stepped-impedance stub-loaded resonator. *In APMC, IEEE,* 2017, 241-243. doi: 10.1109/APMC.2017.8251423
13. Luo, S.; Zhu, L; & Sun, S. (2011). Compact dual-mode triple-band bandpass filters using three pairs of degenerate modes in a ring resonator. *IEEE Trans. Microwave T. Techn.* **59**(5), 1222-1229. doi: 10.1109/TMTT.2011.2123106
14. Liu, H; Lei, J; Guan, X; Sun, L; & He, Y. Compact triple-band high-temperature superconducting filter using multimode stub-loaded resonator for ISM, WiMAX, and WLAN applications. *IEEE Trans. App. Super.,* 2013, **23**(6), 99-103. doi: 10.1109/TASC.2013.2279123
15. Ranjan, P; Kishore, N; Dwivedi, VK; Upadhyay, & G; Tripathi, VS. UWB filter with controllable notch band and higher stop band transmission zero using open stub in inverted T-shaped resonator. *In APMCIEEE,*

2017, 817-820.
doi: 10.1109/APMC.2017.8251574

16. Tsai, LC & Hsue, CW. Dual-band bandpass filters using equal-length coupled-serial-shunted lines and Z-transform technique. *IEEE Trans. Microwave T. Techn*, 2004, **52**(4), 1111-1117.
doi: 10.1109/TMTT.2004.825680
17. Mondal, P & Mandal MK. Design of dual-band bandpass filters using stub-loaded open-loop resonators *IEEE Trans. Microwave T. Techn*, 2008, **56**(1), 150-155.
doi: 10.1109/TMTT.2007.912204
18. Kamma, A; Das, R; Bhatt, D; & Mukherjee, J. Multi-Mode Resonators Based Triple Band Notch UWB Filter. *IEEE MWCL,* 2017, **27**(2), 120-122.
doi: 10.1109/LMWC.2017.2649383
19. Wu, YL; Liao, C; Xiong, XZ; & Zhou, HJ. Miniature dual-mode dual-band bandpass filter with improved passbands performance for 2.4/5.2 GHz WLAN application. *MOTL,* 2014, **56**(5), 1235-1238.
doi: 10.1002/mop.28299
20. Chen, WY; Weng, MH; & Chang, SJ. A new tri-band bandpass filter based on stub-loaded step-impedance resonator. *IEEE MWCL,* 2012, **22**(4), 179-181.
doi: 10.1109/LMWC.2012.2187884
21. Pal, S; Stevens, CJ; & Edwards DJ. Compact parallel coupled HTS microstrip bandpass filters for wireless communications. *IEEE Trans. Microwave T. Techn.,* 2006,**54**(2), 768-775.
doi: 10.1109/TMTT.2005.862623
22. Mittal, Gaurav & Pathak, NP. Design, analysis and characterisation of spoof surface plasmon polaritons based wideband bandpass filter at microwave frequency. *Def. Sci. J.,* 2018, **68**(3), 300.
doi: 10.14429/dsj.68.11981
23. Tripathi, S; Pathak, NP; & Parida M. A Compact Reconfigurable Multi-mode Resonator-based Multi-band Band Pass Filter for Intelligent Transportation Systems Applications. *Def. Sci. J.,* 2018; **68**(6), 547-552.
doi: 10.14429/dsj.68.12769
24. Hong, JS & Lancaster, MJ. Microstrip filters for RF/ microwave applications. *Joh. Wil. & Sons*; 2004.
doi: 10.1002/9780470937297.
25. Guo, Jian-Hui; Sai-Wai, Wong; Jing-Yu Lin; Yin, Li; Long, Zhang; Lei, Zhu; Ze-Ming Xie; & Yejun, He. A continuously tunable bandpass filter using distilled water based on multiple-mode resonator. *IEEE MWCL,* 2020, **30**(5), 477-480.
doi: 10.1109/LMWC.2020.2982806
26. Wu, Yi-Wen; Zhang-Cheng, Hao; Rong, Lu; & Jia-Sheng, Hong. A high-selectivity D-band mixed-mode filter based on the coupled overmode cavities. *IEEE Trans. Microwave T. Techn.,* 2020, 68(6), 2331-2342.
doi: 10.1109/TMTT.2020.2977903
27. Cao, Zilan; Xiaojun, Bi & Qinfen, Xu. Reflection less triple-band BPF by reused even-mode resonances of multi-mode resonator. *Elect. Lett*., 2019, **55**(10), 609-11.
doi: 10.1049/el.2019.0439
28. Xie, Hao-Wei; Kang, Zhou; Chun-Xia, Zhou; & Wen Wu. Stopband-improved SIW triplexes and triple-band filters using alternately cascaded triple-and single-mode cavities. *IEEE Access*, 2019, **7**, 56745-56752.
doi: 10.1109/ACCESS.2019.2913713

CONTRIBUTORS

Dr Shivesh Tripathi, received his PhD from Indian Institute of Technology, Roorkee, India in 2019. Currently he is working as Associate Professor in the Department of Electrical and Electronics Engineering, Galgotias College of Engineering and Technology, Gr. Noida, India. His current areas of research are Microwave and Millimeter Wave Technology, Microstrip Antennas, MIMO/Diversity Antennas for 5G and IoT application, RF Integrated Circuits and Systems, Software defined radios and Intelligent Transportation Systems. He has published many research articles in International Journals and Conference Proceedings.

In the current study, he is to conceived of the presented idea its simulation and measurement.

Dr Baibaswata Mohapatra received the PhD from National Institute of Technology, Allahabad, in 2011. He is presently working as a Professor & Dean, School of Electrical, Electronics and Communication Engineering, Galgotias University. His area of interest includes Communication and Networking and published several research papers in International Journals and conferences.

Contribution in the current study, he provided inputs in simulation.

Dr Prabhakar Tiwari did BE in Electrical Engineering from MMMEC, Gorakhpur, MTech in Power Systems Engineering from IIT, Delhi and PhD from JMI Central University. Currently he is Associate Professor, EE Department, Madam Mohan Malaviya University of Technology, Gorakhpur, India. His major field of interest includes Renewable Energy, Re-structuring, Deregulation, Power System Pricing, Power System Stability, Smart Grid and Quality in Technical Education. He has written 2 books and more than 70 papers in the different National & International Journals and Conferences.

Contribution in the current study, he provided inputs in measurements.

Dr V.S.Tripathi received his MTech (Digital Systems) and PhD from Motilal Nehru National Institute of Technology Allahabad, Prayagraj. Currently working as Professor in the Department of Electronics & Communication Engineering, Motilal Nehru National Institute of Technology Allahabad, Prayagraj. His current research interests are: Linear and Nonlinear integrated circuits and systems at RF frequencies, Non-invasive RF Sensor Systems, Near-Field Imaging for medical applications, intelligent transportation systems, SDR, Neural Networks and Cognitive radio. He has written many book chapters and more than 70 papers in the International Journals and International Conferences.

In the current study, he provided inputs in manuscript writing.